DISCOVERY OF ASSOCIATED ABSORPTION LINES IN AN X-RAY WARM ABSORBER: *HUBBLE SPACE TELESCOPE* FAINT OBJECT SPECTROGRAPH OBSERVATIONS OF MR 2251−178[1]

Eric M. Monier and Smita Mathur

Department of Astronomy, Ohio State University, 140 West 18th Avenue, Columbus, OH 43204; monier@astronomy.ohio-state.edu, smita@astronomy.ohio-state.edu

AND

Belinda Wilkes and Martin Elvis

Harvard-Smithsonian Center for Astrophysics, 60 Garden Street, Cambridge, MA 02138
Received 2001 February 20; accepted 2001 May 14

ABSTRACT

The presence of a "warm absorber" was first suggested to explain spectral variability in an X-ray spectrum of the radio-quiet quasi-stellar object (QSO) MR 2251−178. A unified picture, in which X-ray warm absorbers and "intrinsic" UV absorbers are the same, offers the opportunity to probe the nuclear environment of active galactic nuclei. To test this scenario and understand the physical properties of the absorber, we obtained a UV spectrum of MR 2251−178 with the Faint Object Spectrograph on board the *Hubble Space Telescope* (*HST*). The *HST* spectrum clearly shows absorption due to Lyα, N v, and C iv, blueshifted by 300 km s^{-1} from the emission redshift of the QSO. The rarity of both X-ray and UV absorbers in radio-quiet QSOs suggests these absorbers are physically related, if not identical. Assuming the unified scenario, we place constraints on the physical parameters of the absorber and conclude the mass outflow rate is essentially the same as the accretion rate in MR 2251−178.

Subject headings: quasars: absorption lines — quasars: individual (MR 2251−178) — ultraviolet: galaxies

1. INTRODUCTION

Absorption because of O vii and O viii in the X-ray and O vi in the UV can in some cases be modeled by a single UV/X-ray absorber (Mathur 1994; Mathur, Wilkes, & Elvis 1998), offering a unique way to determine the physical conditions of the absorbing material in active galactic nuclei (AGNs). As more X-ray/UV absorbers have been found (e.g., Mathur 1994; Mathur, Elvis, & Wilkes 1995b; Mathur, Elvis, & Singh 1995a; Mathur, Wilkes, & Aldcroft 1997; Shields & Hamann 1997; Mathur et al. 1998; Hamann, Netzer, & Shields 2000), it has become clear these share common characteristics. Although not all of these absorbers can be readily modeled by a single zone, all are composed of highly ionized, low-density, high column density, outflowing gas sitting outside the broad emission line region (BELR). The X-ray/UV absorbers are therefore an important nuclear component of AGNs, representing a wind or outflow carrying away significant kinetic energy at a mass-loss rate comparable to the accretion rate needed to power the AGN (Mathur et al. 1995b). The properties of these absorbers can be invoked in AGN models developed to explain such outflows (see Elvis 2000 and references therein) and will aid in expanding such models into a wider unification scenario (Elvis 2000).

It remains to be determined how common X-ray/UV absorbers are. In a sample of eight Seyfert galaxies, Crenshaw et al. (1999) found that six of them showed both UV and X-ray absorption, strengthening the UV/X-ray connection. The question remains whether X-ray absorbers are physically related to UV absorbers in all AGNs (two of the Seyfert galaxies of the Crenshaw et al. sample were not X-ray warm absorbers and showed no UV absorption) or, if not, in what fraction of cases does the unified model apply. To help answer these questions, we initiated a *Hubble Space Telescope* (*HST*) program to search for UV absorption in two radio-quiet quasi-stellar objects (QSOs) with known X-ray warm absorbers.

Mathur et al. (1998) reported UV absorption in the first of these objects, PG 1114+445. Here we present the detection of UV absorption in our second candidate, MR 2251−178, a low-redshift ($z_{em} = 0.0640$) radio-quiet QSO. In addition to being the first X-ray–selected QSO (Ricker et al. 1978), MR 2251−178 was the object for which Halpern (1984) originally suggested the presence of partially ionized, optically thin material: the X-ray warm absorber.

In § 2 we describe the *HST* observations and the analysis of the UV absorption lines. Section 3 relates the UV absorption to the X-ray absorption seen in *ASCA* data analyzed by Reynolds (1997) and presents some simple physical quantities on the basis of the assumption that the UV and X-ray absorbers are the same. We present our conclusions in § 4.

2. THE *HST* SPECTRA

On 1996 February 2, MR 2251−178 was observed using three gratings of the Faint Object Spectrograph (FOS) on board *HST*. The target was centered in the 1″ circular aperture through a four-step peak-up sequence to ensure a pointing accuracy of 0″.12. Two exposures totaling 5740 s were obtained using the G130H grating and the blue side of the detector. The exposures using the red side and the G190H and G270H gratings were 1730 and 300 s, respectively.

The data were reduced using the standard pipeline processing and calibration files, and the individual G130H

---

[1] Based on Observations with the NASA/ESA *Hubble Space Telescope*, obtained at the Space Telescope Science Institute, which is operated by AURA, Inc., under NASA contract NAS 5-26555.

spectra were combined. The final spectra are shown in Figure 1. Absorption lines of Lyα, C IV, and N V can be clearly seen, as predicted from the X-ray/UV models. The strong absorption lines of Lyα and C IV are superposed on the emission lines of Lyα and C IV. Weaker absorption owing to the N V doublet is seen against the continuum; no measurable N V emission is present. The spectra do not show absorption by low-ionization Mg II, indicating the UV absorber is highly ionized.

There is an inherent uncertainty involved in measuring an absorption line lying on top of a broad emission-line profile because the unabsorbed shape of the emission line is unknown. We therefore used two methods to measure the line equivalent widths (EWs) as in Mathur et al. (1998). We made an initial measurement using the IRAF SPLOT task to fit Gaussians across the absorption in the emission-line profiles. A single Gaussian was used for Lyα and N V lines, and the C IV doublet was deblended into two Gaussians. Results for the EWs and FWHMs are listed in Table 1. We estimate the errors on the EWs for Lyα and C IV to be

~40%. The continuum is more readily determined on either side of the N V lines; hence, the error on the SPLOT measurement is estimated at ~10%. The C IV and N V doublet ratios are both ≈1.7, so the doublets may be partially saturated, although not as severely as in PG 1114+445. Higher resolution spectra would be needed to address the degree of saturation. Also, although it is probable the individual lines will break into multiple components at higher resolution (Lyα in fact has two components; see § 3.1), we treat them as single lines here.

To obtain a more accurate estimate of the absorption-line EWs, we used the SPECFIT (Kriss 1994) task under STSDAS to simultaneously fit the underlying continuum and the emission- and absorption-line profiles. The continuum was characterized by a simple power law, the emission lines were fitted with multiple Gaussians, and each absorption line was fitted with a single Gaussian. First, the power-law continuum was fitted to featureless parts of the spectrum on either side of the emission lines and the absorption to be measured. The parameters of the power-
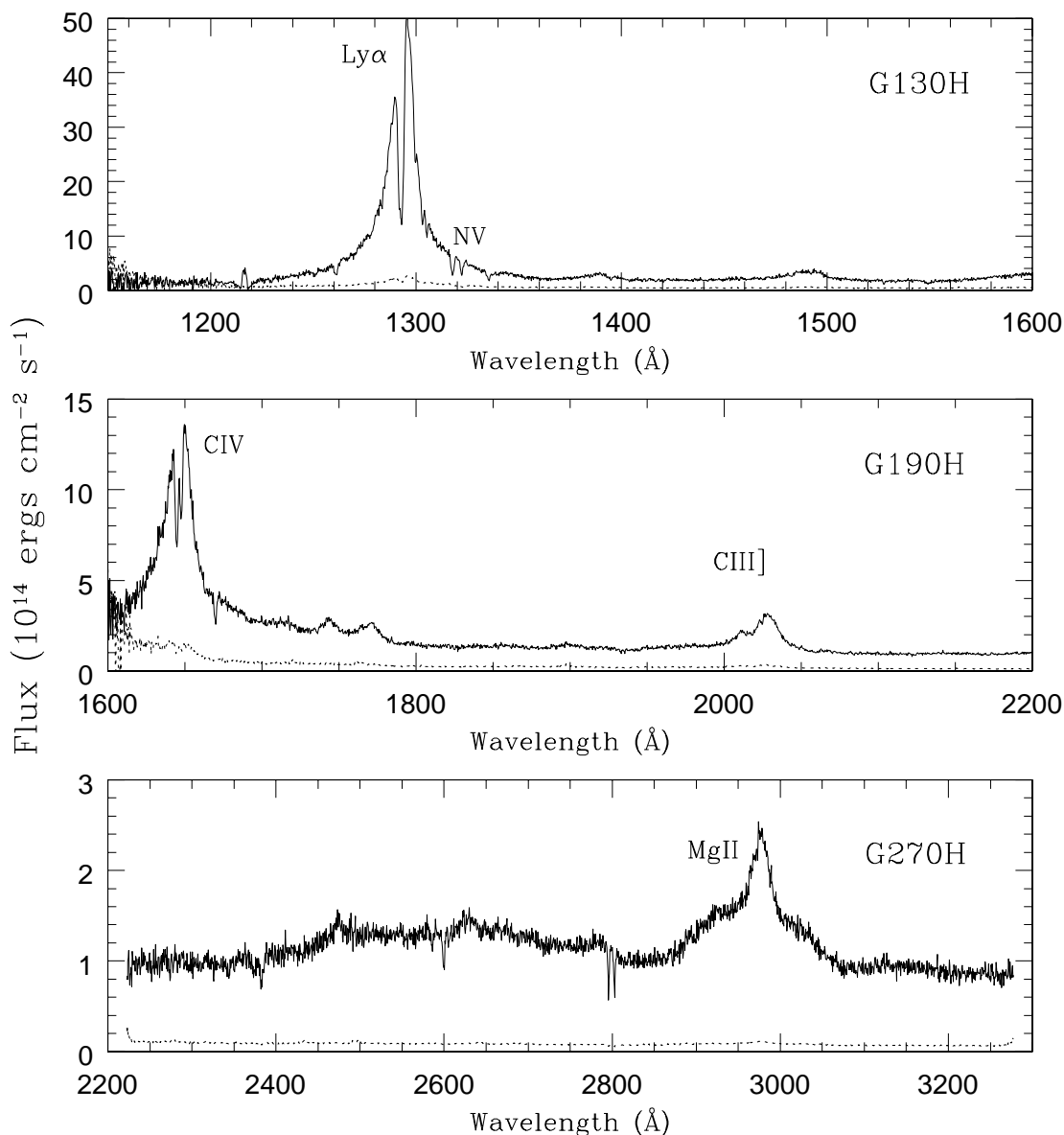

FIG. 1.—*HST* spectrum of MR 2251−178 showing absorption lines of Lyα, N V, and C IV. The lower line on each panel is the error spectrum.

TABLE 1

ABSORPTION-LINE PARAMETERS

LINE	INSTRUMENT	λ_{obs} (Å)	z	EW[a] (Å)		FWHM (km s^{-1})		N_{ion} (cm^{-2})	
				SPLOT	SPECFIT	SPLOT	SPECFIT	Observed[b]	Predicted[c]
Lyα 1215.7	FOS-G130H	1292.6	0.0630	2.22	2.52 ± 0.08	694	754 ± 23	>(3.8–4.4) × 10^{14}	8.4 × 10^{14}
Lyα 1215.7	STIS-G140M	1290.9	0.0619	...	0.26 ± 0.01	...	108 ± 37	(6.4 × 10^{13})[d]	...
Lyα 1215.7	STIS-G140M	1292.3	0.0630	...	1.90 ± 0.01	...	475 ± 24	(6.4 × 10^{14})[d]	...
C IV 1548.2......	FOS-G190H	1644.7	0.0623	1.07	1.09 ± 0.08	434	410 ± 25	>(6–7) × 10^{14}	1.6 × 10^{13}
C IV 1550.8......	FOS-G190H	1647.6	0.0624	0.64	0.80 ± 0.07	399	363 ± 25	...	...
N V 1238.8	FOS-G130H	1317.8	0.0637	1.02	1.14 ± 0.11	382	444 ± 51	>(10–11) × 10^{14}	1.6 × 10^{14}
N V 1242.8	FOS-G130H	1322.2	0.0638	0.61	0.71 ± 0.10	304	325 ± 57	...	...

[a] Rest-frame EW. SPLOT error estimates are 40% on Lyα and C IV, 10% on N V.

[b] FOS values are lower limits from the linear part of the curve of growth. Two numbers correspond to SPLOT and SPECFIT values.

[c] Prediction from photoionization code CLOUDY using "Table AGN" input continuum.

[d] Curve-of-growth measurement.

law continuum—the slope and the normalization—were then fixed in subsequent fits. The parameters of the Gaussians used to fit the emission lines (flux, centroid, FWHM, and skew) and the absorption lines (flux, centroid, and FWHM) were allowed to vary freely. The fits to the Lyα, N V, and C IV emission/absorption profiles are shown in Figure 2, and the corresponding EW and FWHM of the absorption fits are given in Table 1. The results of the SPLOT and SPECFIT methods are qualitatively similar, although the SPECFIT values are systematically larger owing to the higher continuum provided by fitting the emission lines. These differences are unimportant to the discussion.

The observed FWHM of the absorption lines is 1.3–3.0 Å (>300 km s^{-1}) with SPLOT and 1.4–3.3 Å (>320 km s^{-1}) with SPECFIT. For each ion the total absorption is likely resolved given the ≈ 230 km s^{-1} resolution of FOS, so the absorber is dispersed in velocity space. In a higher resolution spectrum, however, the absorption lines may split into multiple components. The average absorption redshift for the five lines is $\langle z \rangle = 0.063$, blueshifted by 300 km s^{-1} from the QSO emission redshift of $z_{em} = 0.0640$ (Bergeron et al. 1983). We expect that O VI absorption is also present, but it lies below the blue cutoff of the G130H grating at the redshift of MR 2251−178.

MR 2251−178 was also observed in 1998 December by J. Stocke with *HST*-STIS (Space Telescope Imaging Spectrograph) over the wavelength range 1250–1300 Å. The Lyα absorption line breaks into a broad component and a narrow component at the ≈ 12 km s^{-1} resolution of the STIS G140M grating. Figure 3 shows the Lyα region and a fit to the absorption profile produced with SPECFIT as described previously. The resulting line centers, EWs, and FWHMs of the two components are listed in Table 1.

3. THE X-RAY/UV ABSORBER

High-ionization UV absorption lines owing to Lyα, N V, and C IV are seen in the *HST* spectrum of MR 2251−178, as predicted by UV/X-ray models. Mathur et al. (1998) estimate the chance probability that a radio-quiet QSO will have both associated UV and X-ray ionized absorption to be $\sim 1.7 \times 10^{-3}$. This strongly suggests the two absorption systems are physically related.

3.1. *Physical Properties of the Ionized Gas*

To explore the possibility that the UV and X-ray absorp-

tion lines arise in the same component of the nuclear material of the AGN, we need to compare the properties of the UV and X-ray absorbers.

We took the measurements of the X-ray absorber in MR 2251−178 from the analysis of *ASCA* data (obtained 1993 November 6) by Reynolds (1997; Komossa 2001 obtains a similar result using *ROSAT* data from the same epoch). The total equivalent hydrogen column density of the X-ray absorber is $N_H = 5 \times 10^{21}$ atoms cm^{-2}, determined by fitting the warm absorber with a one-zone model using the CLOUDY photoionization code (Ferland 1996). Reynolds constrained the optical depths of the O VII/O VIII edges in a simple two-edge model with a power-law continuum ($\alpha = 1.73$). We used these values as an input to CLOUDY to derive the column densities of the UV ions seen in absorption in the *HST* data. The standard "Table AGN" (Mathews & Ferland 1987) continuum (with a resulting ionization parameter of $U = 1.0$)[2] was used with the assumption of solar abundances. The shape of the observed UV continuum of MR 2251−178 (Fig. 1) is consistent with that in "Table AGN." Table 1 lists the CLOUDY predictions for the ionic column densities of H I, N V, and C IV, as derived from the X-ray data.

To compare these predictions to what is observed in the UV, it is necessary to convert the EWs to column densities. As discussed in § 2, the lines may be somewhat saturated; thus, the column densities can be calculated only if the velocity dispersion parameter (*b*-parameter) of the lines is known. If the lines are resolved, then $b \approx 450$ km s^{-1} [$b =$ FWHM$/(4 \ln 2)^{1/2}$; the FWHM is given in Table 1] for Lyα and ≈ 200–270 km s^{-1} for C IV and N V. The X-ray prediction for the column density of hydrogen, $N_{H I} = 8 \times 10^{14}$ cm^{-2}, is therefore about a factor of 2 larger than the minimum value measured in the FOS data ($N_{H I} \approx 4 \times 10^{14}$ cm^{-2}). Agreement between the UV and X-ray values is achieved for $b \approx 200$ km s^{-1}, implying the line breaks into at least two components at higher resolution, as is shown in the STIS data (§ 2).[3] A curve-of-growth analysis using the new *b*-values (~ 65 and ~ 280 km s^{-1}) results in a combined total Lyα column density of $\sim 7 \times 10^{14}$, in good agreement with the X-ray prediction for H I.

[2] *U* is defined as the dimensionless ratio of ionizing photon to hydrogen number density.

[3] A weak feature at ≈ 1295.5 Å may also be Lyα redshifted relative to the quasar, as has been observed in C IV lines of NGC 5548 (Mathur et al. 1999); this feature would not contribute significantly to $N_{H I}$.

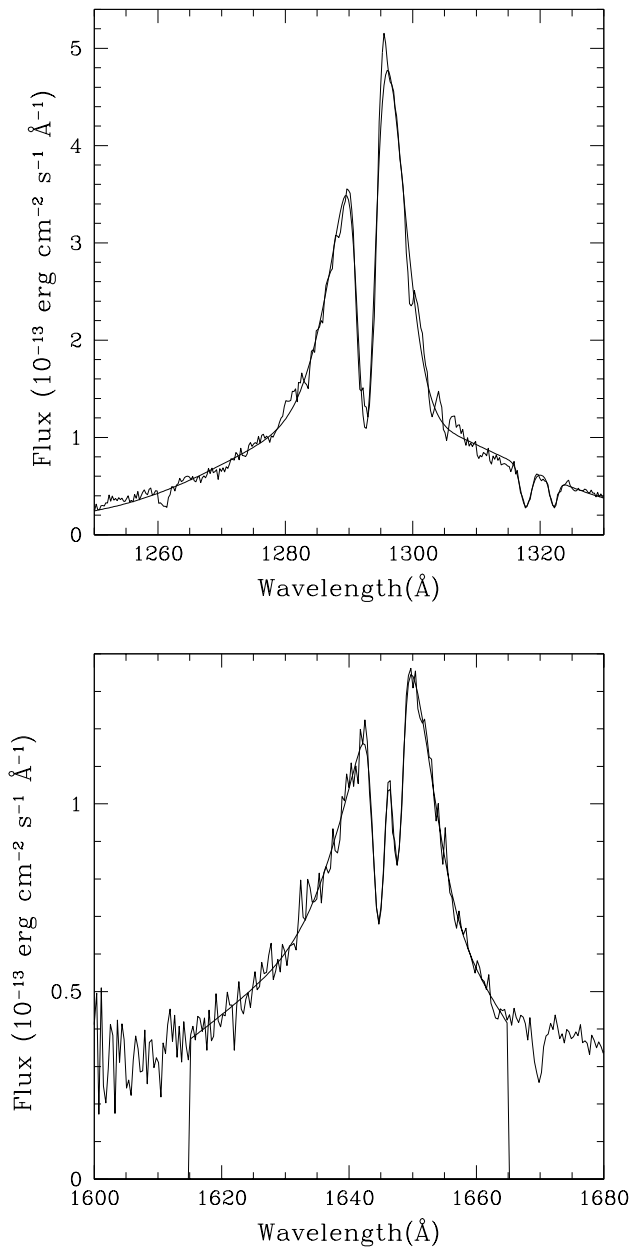FIG. 3.—SPECFIT fit to the *HST*-STIS spectrum of the Lyα absorption line of MR 2251−178. Results of the fit are shown in Table 1.

FIG. 2.—SPECFIT fits to the absorption lines of Lyα and N v (*upper panel*) and C IV (*lower panel*). Results of the fits are shown in Table 1.

(Weymann et al. 1997), NGC 3516 (Kriss et al. 1996; Crenshaw et al. 1999), and NGC 5548 (Mathur et al. 1999; Crenshaw & Kraemer 1999).

Also, note the column densities derived here from the X-ray data are based on the Table AGN continuum. The shape of the actual MR 2251−178 continuum in the unobserved EUV region may greatly affect the predicted column densities (Mathur et al. 1995b). A better match between the observed & predicted values may be obtained if the spectral energy distribution of MR 2251−178 has a different shape. In any case, the X-ray absorber is a large contributor to the absorption measured for C IV and N v in the UV, providing support for the idea that the UV and X-ray absorption is occurring in the same material.

3.2. *Variability*

Halpern (1984) found that the warm absorber in MR 2251−178 was highly variable. *ASCA* data of MR 2251−178 obtained in 1996—near the epoch of the *HST*-FOS data—show a decrease in X-ray intensity from $\log \xi = 1.35$ in 1993 to $\log \xi = 0.96$ in 1996 (Otani, Kii, & Miya 1998), where ξ is an ionization parameter defined as $\xi \equiv L/nr^2$, where n is the number density and r is the distance from the ionizing source with luminosity L. If the ionization parameter U varied similarly, then in 1996 $U = 0.61$ and the X-ray-predicted column densities would be $N_{C IV} = 3.9 \times 10^{14}$ cm^{-2} and $N_{N v} = 2.1 \times 10^{15}$ cm^{-2}, closer to the values measured in the UV data. In this case, $N_{H I}$ grows to 3.4×10^{15} cm^{-2}.

3.3. *Physical Implications*

As noted, the UV absorption indicates the material is flowing outward from the UV/X-ray absorber at ≈ 300 km s^{-1}. With the assumption that the UV and X-ray absorbers are the same, we can determine the physical conditions and mass outflow rate of the absorbing material. We use the total hydrogen column of $N_H = 5 \times 10^{21}$ cm^{-2} and the ion-

The X-ray-predicted values for the N v and C IV are smaller than those calculated from the UV EW measurements. For N v, the X-ray prediction is $N_{N v} = 1.6 \times 10^{14}$ cm^{-2}, while the UV EW measurement gives $N_{H I} = 8 \times 10^{14}$ cm^{-2}, assuming the lines are resolved. Similarly for C IV, the X-ray prediction of $N_{C IV} = 1.6 \times 10^{13}$ cm^{-2} is more than an order of magnitude smaller than the UV measurement of $N_{C IV} \geq 7 \times 10^{14}$ cm^{-2}. The X-ray predictions for $N_{N v}$ and especially $N_{C IV}$ lie on the linear part of the curve of growth. If the UV and X-ray absorbers are the same, we predict these absorbers should break into multiple components—each with lower b—in UV data of higher resolution, leading to values in closer agreement with the X-ray predictions. Kinematically complex UV absorption lines have already been seen in high-resolution data of Mrk 509 (Crenshaw, Boggess, & Wu 1995), NGC 4151
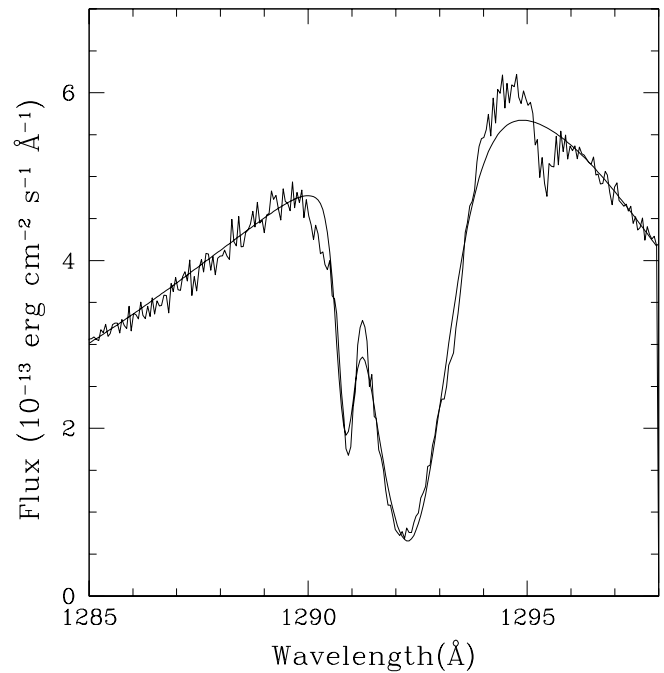
ization parameter $U = 1.0$ from the CLOUDY modeling of the X-ray data. The distance of the absorber from the nucleus is constrained by $U = (Q/4\pi r^2 n_H c)^{1/2}$, where Q is the rate of ionizing photons. We used the *HST* data at 1339 Å rest wavelength to scale the standard Table AGN continuum to the luminosity of MR 2251−178 ($L_{bol} = 5 \times 10^{45}$ ergs s^{-1}). Integrating $L_\nu/(h\nu)$ over $\nu \geq 13.6$ eV gives $Q = 6$ $h^{-2} \times 10^{54}$ s^{-1}, where h is the Hubble constant in units of 100 km s^{-1} Mpc^{-1}. This puts the distance of the absorber from the nucleus at $r = 5.3 \times 10^{18} n_5^{-1/2}$ cm (where $h = 0.75$ and n_5 is the density in units of 10^5 cm^{-3}).

The absorption extends below the continuum level (Fig. 1) and so must cover a substantial fraction of the BELR as well as the continuum source. The absorber may lie outside the BELR or it could also be cospatial with it if most of the emission is beamed from the far side of the BELR. The size of the BELR in MR 2251−178 can be estimated by scaling the BELR of NGC 5548 ($L_{bol} = 5 \times 10^{44}$ ergs s^{-1}) by $L^{1/2}$ (Davidson & Netzer 1979; but see Kaspi et al. 2000). The distance—determined from reverberation mapping—of the BELR from the central continuum in NGC 5548 is $r \simeq 10$ lt-days (Clavel et al. 1991), so the absorber in MR 2251−178 must be at least ~ 32 lt-days, or $r \geq 8.2 \times 10^{16}$ cm from the central source. The corresponding upper limit on the density is then $n < 4.2 \times 10^8$ cm^{-3}. To check the radius estimate, we specified as an input to CLOUDY the luminosity of MR 2251−178 at a rest wavelength of 1339 Å, log $(\nu L_\nu) = 43.78$, and varied the input radius to obtain the ionization parameter output previously. The radius at which $U = 1.0$ was $r = 8.76 \times 10^{16}$ cm. For a covering factor of $f = 0.1$, the column density and particle density of the absorber imply a mass of $M = 152 f_{0.1} n_5^{-1} M_\odot$. The mass outflow rate (Mathur et al. 1995b) would then be $\dot{M}_{out} = 2.9 f_{0.1} M_\odot$ yr^{-1}. (An accretion rate of $\dot{M}_{out} = 0.9 f_{0.1} M_\odot$ yr^{-1} would power MR 2251−178 at 10% efficiency.) The rate of kinetic energy carried away in the flow is $\dot{M} v_{out}^2/2 = 2.6 \times 10^{41}$ ergs cm^{-2} s^{-1}.

4. CONCLUSIONS

The *HST*-FOS UV spectrum of MR 2251−178 exhibits associated high-ionization, UV absorption lines, as predicted from models of the X-ray–ionized absorber. The X-ray/UV absorber is situated outside the BELR or cospatial with it and outflowing with a line-of-sight velocity of ≈ 300 km s^{-1}. The mass outflow rate of 0.9 $M_\odot$ yr^{-1} for a 10% covering factor is equivalent to the accretion rate onto the nuclear black hole.

We expect future higher resolution observations will reveal each of the C IV and N V absorption lines breaking into at least two components.

The rarity of both UV and X-ray absorbers individually in radio-quiet QSOs virtually requires that the X-ray and UV absorbers are closely physically related. The consistency of the column densities obtained from both UV and X-ray data suggests the absorbers are perhaps identical. At a minimum, the X-ray absorber makes a substantial contribution to the absorption seen in the UV. Thus, the absorber in MR 2251−178 satisfies both statistical as well as physical tests of our X-ray/UV absorber model.

REFERENCES

Bergeron, J., Boksenberg, A., Dennefeld, M., & Tarenghi, M. 1983, MNRAS, 202, 125
Clavel, J., et al. 1991, ApJ, 366, 64
Crenshaw, D. M., Boggess, A., & Wu, C.-C. 1995, AJ, 110, 1026
Crenshaw, D. M., & Kraemer, S. B. 1999, ApJ, 521, 572
Crenshaw, D. M., Kraemer, S. B., Boggess, A., Maran, S. P., Mushotzky, R. F., & Wu, C.-C. 1999, ApJ, 516, 750
Davidson, K., & Netzer, H. 1979, Rev. Mod. Phys., 51, 715
Elvis, M. 2000, ApJ, 545, 63
Ferland, G. 1996, Univ. Kentucky, Dept. Phys. Astron. Internal Rep.
Halpern, J. P. 1984, ApJ, 281, 90
Hamann, F. W., Netzer, H., & Shields, J. C. 2000, ApJ, 536, 101
Kaspi, S., Smith, P. S., Netzer, H., Maoz, D., Jannuzi, B. T., & Giveon, U. 2000, ApJ, 533, 631
Komossa, S. 2001, A&A, in press
Kriss, G. A. 1994, in ASP Conf. Proc. 61, Astronomical Data Analysis Software and Systems III, ed. D. R. Crabtree, R. J. Hanisch, & J. Barnes (San Francisco: ASP), 437

Kriss, G. A., Espey, B. R., Krolik, J. H., Tsvetanov, Z., Zheng, W., & Davidsen, A. F. 1996, ApJ, 467, 622
Mathews, W. G., & Ferland, G. J. 1987, ApJ, 323, 456
Mathur, S. 1994, ApJ, 431, L75
Mathur, S., Elvis, M., & Singh, K. P. 1995a, ApJ, 455, L9
Mathur, S., Elvis, M. S., & Wilkes, B. J. 1995b, ApJ, 452, 230
———. 1999, ApJ, 519, 605
Mathur, S., Wilkes, B. J., & Aldcroft, T. 1997, ApJ, 478, 182
Mathur, S., Wilkes, B. J., & Elvis, M. 1998, ApJ, 503, L23
Otani, C., Kii, T., & Miya, K. 1998, in IAU Symp. 188, The Hot Universe, ed. K. Koyama, S. Kitamoto, & M. Itoh (Dordrecht: Kluwer), 436
Reynolds, C. S. 1997, MNRAS, 286, 513
Ricker, G. R., et al. 1978, Nature, 271, 35
Shields, J., & Hamann, F. 1997, ApJ, 481, 752
Weymann, R., Morris, S., Gray, M., & Hutchings, J. 1997, ApJ, 483, 717